

Synthesis of Nanowires in Room Temperature Ambient with Focused Ion Beams

A. Lugstein, C. Schöndorfer, E. Bertagnolli
Institut für Festkörperelektronik, TU Wien,
Floragasse 7, A-1040 Wien

Introduction

Exciting discoveries of essentially new nanostructures, particularly nanowires, have been sparked by a desire to tune the fundamental optical, electronic, mechanical and magnetic properties of materials through rational control of their physical size. Possible applications range from new-generation nanoelectronics [1] to catalysis [2].

Several techniques for the production of various types of nanowires have been reported, such as thermal gas decomposition or laser ablation of powder targets. Most of them are based on the Vapor-Liquid-Solid (VLS) mechanism, in which metal droplets catalytically enhance the growth of nanowires [3]. The liquid alloy cluster serves as a preferential site for adsorption of reactant from the vapor phase and – when supersaturated – as the nucleation site for crystallization. However, there is still an on-going effort in developing synthesis methods with the main goal to grow nanowires at moderate temperatures not to damage preexisting modules and to grow them at a prespecified location while eliminating the requirement of a later assembly process.

Our study differs from all of the previous reports in that an intense focused ion beam initiates the nanowire growth in room temperature ambient without using any additional materials source.

Experimental

All machining experiments were carried out using the Micrion twin lens FIB system (model 2500) equipped with a Ga liquid metal ion source. For patterning, the 50 keV Ga^+ ion beam is scanned in discrete steps across the sample surface at normal incidence. If not mentioned in particular, the processing was done in the single scan mode, thereby each pixel is irradiated only once and the fluence is adjusted by the dwell time the beam remained on each single spot.

The pattern evolution was observed by top-view and cross-sectional Secondary Electron Microscopy (SEM) of cleaved samples, High Resolution Transmission Electron Microscopy (HRTEM) and Electron Dispersive X-ray (EDX) analysis. The chemical composition of the pattern was evaluated by Auger Electron Spectroscopy (AES) using a VG Microlab 310F system enabling a lateral resolution of 20 nm for elemental analysis.

Results

In our approach, we milled holes from the back side through antimony samples, with sufficient initial smoothness, as schematically shown in Fig. 1(a). Remarkably nanowire formation was observed on both sides of the sample, i.e. at the site of the impinging

beam as well as at the plane where the FIB leaves the sample. As FIB milling is done close to the edge of the sample some nanowires extend over the rim of the sample as shown in the SEM image in Fig. 1(b). Thus, enabling HRTEM investigations and Energy Disperse X-ray EDX analysis, of undisturbed nanowires as illustrated in Fig. 1. EDX analysis performed in such a way on individual nanowires proved that the wires consist of pure antimony (left inset in Fig. 1(b)). The Cu signal is an artifact originating from the TEM copper grid. The HRTEM image revealed that the as grown nanowires are amorphous with remarkably uniform diameters in the range of about 25 nm along their entire length (right inset in Fig. 1(b)). Particularly we have investigated the tips of the wires. Neither compositional variations nor solidified catalytic particles, which are characteristic features of a VLS controlled growth mechanism, have been observed on any of the Sb nanowires.

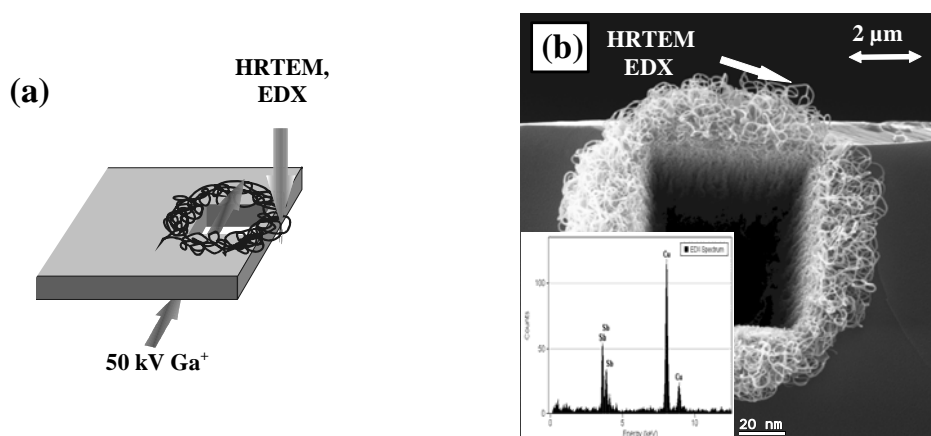


Fig. 1: (a) Schematic illustration of FIB based approach used to synthesize nanowires drilling a hole from the back side through the sample. (b) SEM image of a $5 \times 5 \mu\text{m}^2$ wide hole milled through the sample. The insets show a typical EDX spectrum from an individual nanowire and the HRTEM image of such synthesized wires.

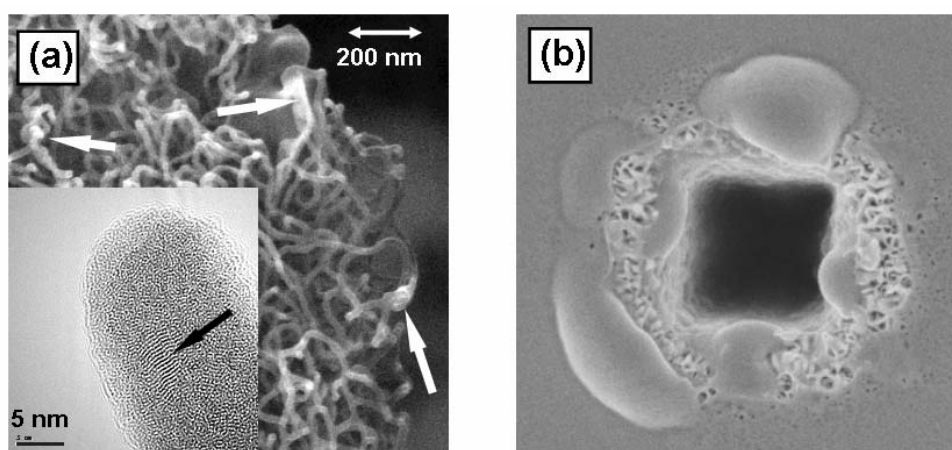


Fig. 2: (a) Low magnified SEM image of the nanowires observed on GaSb after FIB hole milling through the sample. The inset shows a high resolution TEM image of the tip of an isolated GaSb wire with a diameter around 25 nm. (b) SEM image of a hole milled in GaSb with a 30 kV focused Ga^+ ion beam.

For GaSb as substrate material FIB exposure leads to the formation of a cellular structure of columnar tangled rods and precipitations embedded within the porous network of nanowires (see SEM image in Fig. 2(a)). AES measurements revealed that the precipitations marked by the white arrows in Fig. 2(a) appear to be pure Ga. HRTEM investigations (inset of Fig. 2(a)) proved that the roughly 25 nm thick wires show mostly an amorphous structure. For some wires a few regions with a diameter up to 5 nm with crystallographic ordering are visible, indicated by the black arrow. The lattice fringes distance observed in the region marked by the black arrow is 0.35 nm and corresponds with the {111} planes in bulk GaSb with cubic Zinkblende structure. The elemental composition of the nanowires investigated using EDX revealed an almost ideal 1:1 stoichiometry of Ga and Sb independent of the morphology. For beam energies of 30 keV or lower, formation of nanowires could be observed neither for GaSb nor Sb substrates. Fig. 2(b) shows the SEM image of the GaSb surface after 30 kV FIB exposure. The droplet-like features surrounding the FIB milled hole are Ga droplets as determined by AES measurements.

In accordance with the catalytic VLS approach we suppose that the formation of GaSb nanowires necessitates a catalytic particle, mostly a eutectic alloy, with a low melting point. In our approach we suppose that Ga droplets are formed in situ during FIB exposure (Fig. 3(a) - process step 1). As we have recently reported, FIB milling of GaAs leads to the formation of Ga droplets on the surface [4]. For FIB exposure with the 30 keV beam we have also observed in-situ migration of Ga precipitations on the GaSb surface. We assume that exposing the substrate to the 50 keV Ga⁺ ion beam leads to material decomposition due to physical sputtering. The excess Ga atoms because of enhanced diffusion agglomerate into Ga-rich precipitations (process step 1). Due to the low melting point of Ga and high energy injection during FIB milling with the 50 keV beam, these precipitations behave like a liquid. Decomposed material from the substrate – diffusing on the surface – is adsorbed and dissolved by the Ga containing clusters (process step 2). Finally, when the concentration of the solved materials exceeds supersaturation, nucleation sites will be formed and initiate the growth of the coexisting solid GaSb phase (process step 3). Nanowire growth from the base continues as long as the droplet remains in a liquid state and reactant is available. In accordance with the phase diagram shown in Fig. 3(b) precipitation of GaSb continues at the liquid-solid as long as the catalytic particle remains in a liquid state and reactant is available.

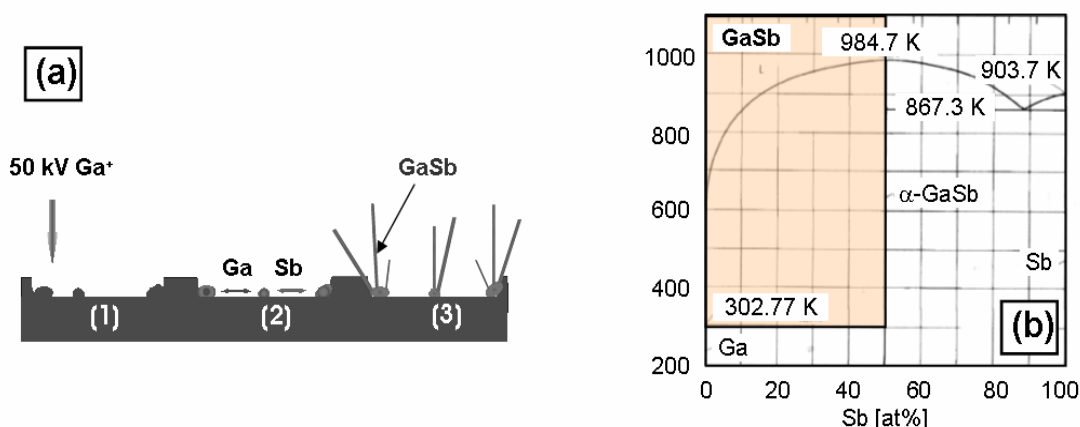


Fig. 3: (a) The proposed growth model; (b) The phase diagram (after Landolt-Börnstein, New Series IV/5) of the binary Ga-Sb system illustrates the thermodynamics of the nanowire growth.

The formation of pure Sb nanowires could be discussed straightforward by examining the Sb rich part of the binary Ga-Sb phase diagram (Fig. 3(b)). Within the framework of our approach, FIB processing of the Sb substrate produces mobile Ga and Sb species on the surface that rapidly agglomerate forming Sb-rich nanoclusters. In case of the Sb substrate Ga is introduced only by the FIB and the concentration of these clusters is somewhere in the right-most part, i.e. the Sb-rich region, of the phase diagram. Again due to supersaturation of the nanocluster, the coexisting pure Sb phase precipitates as nanowires.

At present, we do not understand the origin of the tangling of the nanowires although we note that extensive tangling has been observed previously in Ga based VLS processes [5]. The authors stated also that Ga droplets could simultaneously catalyze the growth of hundreds of thousands of nanowires. Additionally we want to mention that in contrast to the conventional VLS mechanism the growth rate for our approach is extremely high. As the whole FIB processing takes only a few seconds, growth rate must be in the range of a few 100 nm/s.

Conclusion

According to our experimental results, we assume that at least two key parameters are required to induce nanowire formation by an intense FIB. One should use an equilibrium phase diagram to choose a substrate that can form a liquid alloy with Ga. Even when FIB-induced nanowire growth occurs far-off the thermodynamic equilibrium, known phase diagrams can be used to choose a specific composition (catalyst – nanowire material) so that there is coexistence of liquid alloy and solid material. Second, a sufficiently high beam energy to ensure that the liquid alloy is formed during the FIB processing.

The above studies illustrate the potential of our approach for synthesis of nanowires in room temperature ambient without using a gas-type source. We suppose that our approach should not be limited solely to the materials discussed here – other substrates or sources of the ion beam should extend this method to other materials.

Acknowledgements

This work is partly funded by the Austrian Science Fund (Project No. 18080-N07). The authors would like to thank the Center for Micro- and Nanostructures (ZMNS) for providing the clean-room facilities. The financial support from the Austrian Society for Micro- and Nanoelectronics (GMe) is gratefully acknowledged.

References

- [1] A. O. Orlov, I. Amlani, G. H. Bernstein, C. S. Lent, G. L. Snider, *Science* 277, 928 (1997); A. B. Greytak, L. J. Lauhon, M. S. Gudiksen and C. M. Lieber, *Appl. Phys. Lett.* 84, 4176 (2004); A. P. Alivisatos, *Science* 271, 933 (1996); S. Sun, C. B. Murray, D. Weller, L. Folks, A. Moser, *Science* 287, 1998 (2000).
- [2] M. Valden, X. Lai, D. W. Goodman, *Science* 281, 1647 (1998).
- [3] R. S. Wagner, W. C. Ellis, *Appl. Phys. Lett.* 4, 89 (1964).
- [4] A. Lugstein, B. Basnar, E. Bertagnolli, *J. Vac. Sci. Technol. B* 22, 888 (2004).
- [5] Z. W. Pan, Z. R. Dai, C. Ma, Z. L. Wang, *J. Am. Chem. Soc.* 124, 1817 (2002).